Supporting information – New Journal of Chemistry

Detection of phosphates in water utilizing Eu^{3+}-mediated relay mechanism

Sepideh Farshbaf,[a] Kaustav Dey,[a] Wakana Mochida,[b] Masashi Kanakubo,[b] Ryuhei Nishiyabu,[b] Yuji Kubo,*[b] and Pavel Anzenbacher, Jr.*[a]

[a] Department of Chemistry, Bowling Green State University, Bowling Green, OH 43403, USA E-mail: pavel@bgsu.edu

[b]Department of Applied Chemistry, Graduate School of Urban Environmental Sciences, Tokyo Metropolitan University, Tokyo 192-0397 (Japan)
E-mail: yujik@tmu.ac.jp
Email: ryuhei@tmu.ac.jp

Table of Contents

1. General

The carboxamidequinoline based ligands have been synthesized in Dr. Kubo group and characterized by ^{1}H NMR, ^{13}C NMR, MS, and elemental analysis.[1] Standard laboratory techniques were performed in the synthesis. All chemicals were analytical grade and they were used without purification. NMR spectra were taken by a Bruker Avance 500 MHz NMR spectrometer. In ^{1}H and ^{13}C NMR measurements, chemical shifts (δ) are reported downfield from the chemical shift of tetramethylsilane as an internal standard. Mass spectrometry (MS) was performed by using a fast atom bombardment (FAB) mass spectrometer (JEOL JMS-700) and an atmospheric pressure chemical ionization (APCI) and electrospray ionization (ESI) mass spectrometer (Bruker micrO-TOF). m-Nitrobenzylalcohol was used as a matrix for FAB-MS and Tuning-Mix was used as a calibration standard for APCI and ESI-MS. Elemental analyses were performed on an Exeter Analytical, Inc. CE-440F elemental analyzer. Absorption spectra were recorded using an Agilent Technologies Cary 60. Fluorescence emission spectra and job-plot stoichiometry determinations were acquired using an Edinburgh single photon counting spectrofluorimeter (FLSP 920). The quantum yields were recorded by using a Hamamatsu Quantaurus QY-C11347 absolute quantum yield integrating sphere. Fourier-Transform Infrared (FTIR) Spectra were obtained on a Thermo Scientific Nicolet iS5 Fourier transform infrared spectrometer. The attenuated total reflection method was used. All the optical measurements were performed using a quartz cuvette with a path length of 1 cm at room temperature. All measurements were performed in HPLC grade Methanol and 0.2 and 2.5% spectrophotometric grade DMSO. The stock sloutions for titration of **1**, **2** and **3** with $Eu(OTf)_3$ were prepared in high concentrations in ependorf

tubes including 1 mM ligands mixing with 0 – 8 mM $Eu(OTf)_3$ for **1, 2** and 0 – 5 mM $Eu(OTf)_3$ for **3**. The stock solutions were incubated for 40 minutes before measurement. All fluorescence measurements were repeated at least three times.

The binding constants were determined by a nonlinear least-square analysis using a 1:1 complexation model which is supported by the random distribution pattern of residuals obtained from the Bindfit from Supramolecular.org (Supramolecular.org - Binding Constant Calculators | Supramolecular).

2. Synthesis of ligands 1-3 and intermediate 9

The syntheses of 2-amino-*N*-(quinolin-8-yl) acetamide **(6)**[2], 2-(benzo[d]thiazol-2-yl)-4-methylphenol **(8)**[3], and 3-(benzo[d]thiazol-2-yl)-2-hydroxy-5-methylbenzaldehyde **(9)**[1] were performed according to the reported procedures.

Synthesis of 2-((2-hydroxybenzyl)amino)-*N*-(quinolin-8-yl)acetamide (1)

2-Amino-*N*-(quinolin-8-yl) acetamide (0.96 g, 3.4 mmol) and salicylaldehyde (0.41 mL, 3.9 mmol) were dissolved in dry ethanol (60 mL), and the solution was stirred for 6 h at room temperature. The mixture was then cooled to 0 °C, and sodium borohydride (0.31 g, 9.0 mmol) in dry ethanol (50 mL) was added to the mixture. The resulting mixture was allowed to stir at room temperature under a nitrogen atmosphere for 4 h. The reaction mixture was poured into 0.1 M hydrochloric acid (20 mL) and then ethyl acetate (150 mL) was added to the aqueous mixture. The organic layer was separated and dried over sodium sulfate. After evaporation of the filtrate *in vacuo*, the residue was recrystallized from ethyl acetate to give 0.48 g of 1 as a white solid in 45% yield. ^1H

NMR (500 MHz, $CDCl_3$) δ (ppm): 10.04 (s, 1H), 8.80 (dd, *J* = 4.20; 1.65 Hz, 1H), 8.76 (dd, *J* = 6.60; 2.20 Hz, 1H), 8.18 (dd, *J* = 1.65; 8.23 Hz, 1H), 7.58-7.54 (m, 2H), 7.47 (dd, *J* = 4.25; 8.30 Hz, 1H), 7.21 (td, *J* = 1.43; 7.75 Hz, 1H), 7.04 (d, *J* = 7.45 Hz, 1H), 6.90 (dd, *J* = 8.10; 0.90 Hz, 1H), 6.81 (td, *J* = 7.40; 1.10 Hz, 1H), 4.11 (s, 2H), 3.64 (s, 2H). ^{13}C NMR (126 MHz, $CDCl_3$) δ (ppm): 168.6, 157.85, 148.41, 138.32, 136.4, 133.79, 129.11, 129.05, 127.97, 127.33, 122.16, 122.02, 121.79, 119.39, 116.69, 116.63, 52.29, 51.67. FAB-MS: *m/z* = 308 $[M+H]^+$ (Calculated mass: 308). Elemental analysis calcd (%) for $C_{18}H_{17}N_3O_2$: C 70.34, H 5.58, N 13.67; found: C 70.04, H 5.54; N 13.44.

Synthesis procedure of 3-(benzo[d]thiazol-2-yl)-2-hydroxy-5-methylbenzaldehyde (9)

2-(Benzo[d]thiazol-2-yl)-4-methylphenol (**8**) (0.51 g, 2.1 mmol) and hexamethylenetetramine (0.61 g, 4.3 mmol) were dissolved in trifluoroacetic acid (40 mL). Then the reaction mixture was refluxed at 80 °C for overnight under a nitrogen atmosphere, poured into 1 M NaOH aq. (400 mL), and extracted with CH_2Cl_2 (100 mL). The organic layer was washed with NaCl aq. (100 mL), dried over Na_2SO_4 and filtered off. After evaporation in vacuo, the residue was chromatographed on silica gel (Wacogel C-300) using dichloromethane/*n*-hexane = 1:1 (v:v) to give 0.44 g of **9** as a yellow solid in 77% yield. ^1H NMR (500 MHz, $CDCl_3$) δ (ppm): 13.02 (s, 1H), 10.50 (s, 1H), 8.03 (d, *J* = 8.10 Hz, 1H), 7.95 (d, *J* = 7.95 Hz, 1H), 7.91 (s, 1H), 7.72 (s, 1H), 7.55 (ddd, *J* = 7.75, 7.65 and 1.23 Hz, 1H), 7.45 (ddd, *J* = 7.60, 7.70 and 1.08 Hz 1H), 2.41 (s, 3H). FAB-MS: *m/z* = 270 [M+H] (Calculated mass: 270).

Synthesis of (Z)-2-((3-(benzo[d]thiazol-2-yl)-2-hydroxy-5-methylbenzyl)imino)-*N*-(quinolin-8-yl)acetamide (2)

2-Amino-*N*-(quinolin-8-yl) acetamide (0.15 g, 0.74 mmol) and 3-(benzo[d]thiazol-2-yl)-2-hydroxy-5-methylbenzaldehyde **(9)** (0.20 g, 0.74 mmol) were dissolved in dry ethanol (50 mL), and the solution was refluxed at 80 °C under a nitrogen atmosphere for 3 h. After cooling to room temperature, a yellowish precipitate was collected to give 0.29 g of **2** as a yellow solid in 87% yield. ^{1}H NMR (500 MHz, $CDCl_3$) δ (ppm): 12.69 (s, 1H), 11.47 (s, 1H), 8.83-8.85 (m, 2H), 8.13 (d, *J* = 8.20 Hz, 1H), 7.97 (d, *J* = 7.75 Hz, 1H), 7.80 (s, 1H), 7.52-7.58 (m, 3H), 7.41-7.46 (m, 3H), 4.64 (s, 1H), 2.49 (s, 3H). ^{13}C NMR (126 MHz, $CDCl_3$): δ (ppm) 167.7, 156.7, 151.9, 148.5, 138.8, 136.2, 134.6, 134.1, 133.4, 132.6, 128.6, 128.6, 127.3, 126.4, 125.2, 122.5, 121.9, 121.7, 121.5, 121.2, 119.6, 116.5, 111.1, 77.7, 63.6, 63.5. APCI-MS: *m/z* = 453 $[M+H]^+$ (Calculated mass: 453). Elemental analysis calcd (%) for $C_{26}H_{20}N_4O_2S$: C, 69.01, H 4.45, N 12.38; found: C 68.81, H 4.45, N 12.36.

Synthesis of 2-((3-(benzo[d]thiazol-2-yl)-2-hydroxy-5-methylbenzyl)amino)-*N*-(quinolin-8-yl)acetamide (3)

2-Amino-*N*-(quinolin-8-yl) acetamide (0.41 g, 1.5 mmol) and 3-(benzo[d]thiazol-2-yl)-2-hydroxy-5-methylbenzaldehyde **(9)** (0.31 g, 1.5 mmol) were dissolved in dry ethanol (60 mL), and the solution was refluxed at 80 °C for 2 h under a nitrogen atmosphere. The mixture was cooled to 0 °C, and sodium borohydride (0.23 g, 6.1 mmol) in dry ethanol (30 mL) was added to the mixture. Then the mixture was allowed to stir at room temperature for 2 h under a nitrogen atmosphere. The resulting mixture was poured into

0.1 M hydrochloric acid (10 mL) and ethyl acetate (100 mL) was added to the aqueous mixture. The organic layer was dried over sodium sulfate. After evaporation of the filtrate *in vacuo*, recrystallization of the residue from ethyl acetate afford 0.45 g of **3** as a light yellow solid in 66% yield. ^{1}H NMR (500 MHz, $CDCl_3$) δ (ppm) : 12.69 (s, 1H), 11.47 (s, 1H), 8.83-8.85 (m, 2H), 8.25 (dd, *J* = 8.20; 1.65 Hz, 1H), 7.93 (dd, *J* = 17.05; 7.95 Hz, 1H), 7.49-7.56 (m, 3H), 7.39-7.43 (m, 3H), 7.30 (s, 1H), 4.05 (s, 2H), 3.59 (s, 2H), 2.56 (s, 1H), 2.35 (s, 3H). ^{13}C NMR (126 MHz, $CDCl_3$): δ (ppm) 170.7, 169.4, 154.3, 151.8, 148.5, 139.1, 136.1, 134.6, 134.6, 132.7, 128.3, 128.1, 127.6, 127.5, 127.3, 126.7, 125.5, 122.1, 121.6, 121.5, 121.4, 116.6, 116.3, 52.9, 49.4, 20.5. FAB-MS: *m/z* = 455 $[M+H]^+$ (Calculated mass: 455). Elemental analysis: calcd (%) for $C_{26}H_{22}N_4O_2S$: C 68.70, H 4.88, N 12.33; found: C 68.64, H 4.93, N 12.27.

3. Characterization of ligands 1-3 and intermediate 9

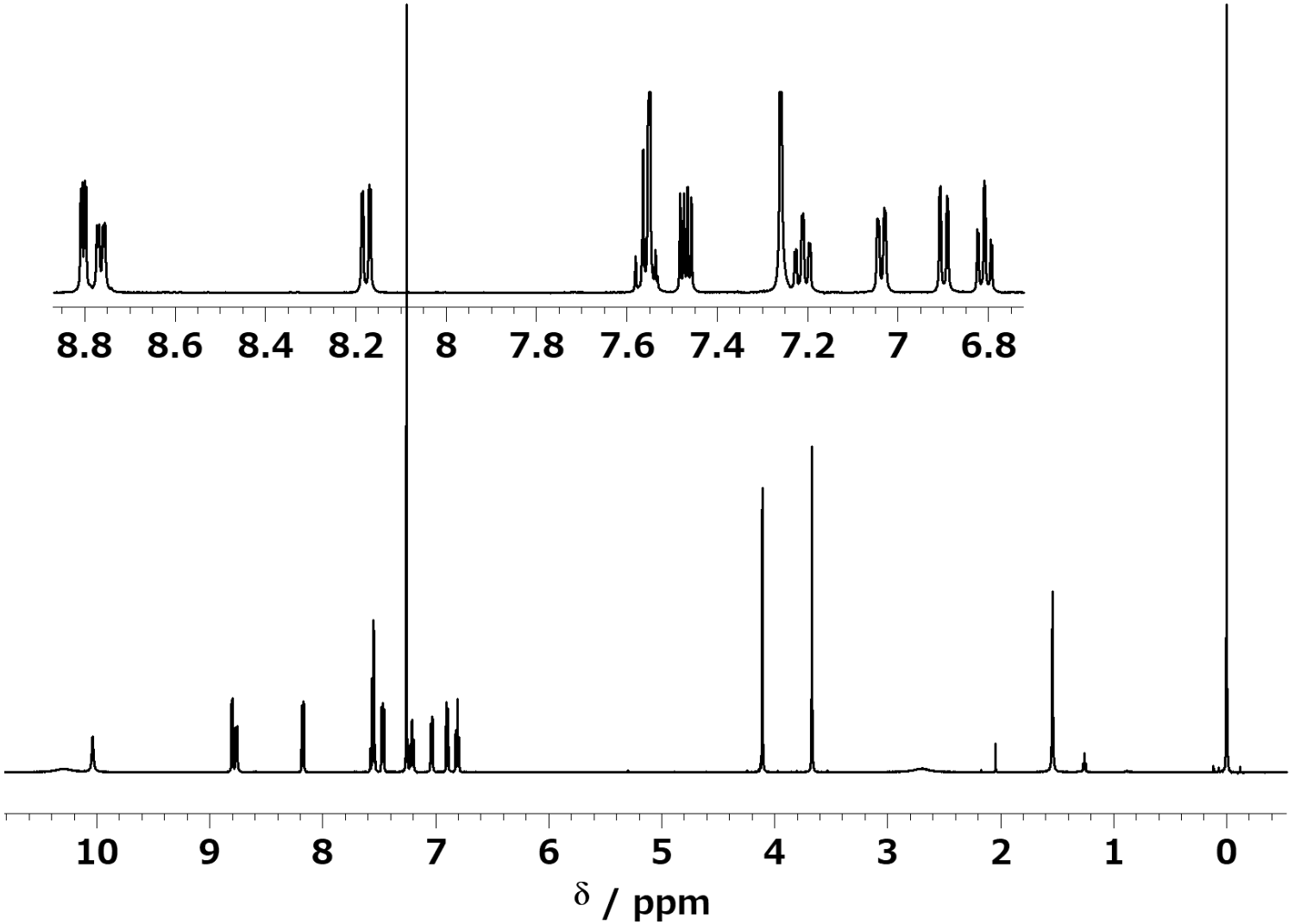

Figure S1. ^{1}H NMR spectrum of **1** in $CDCl_3$.

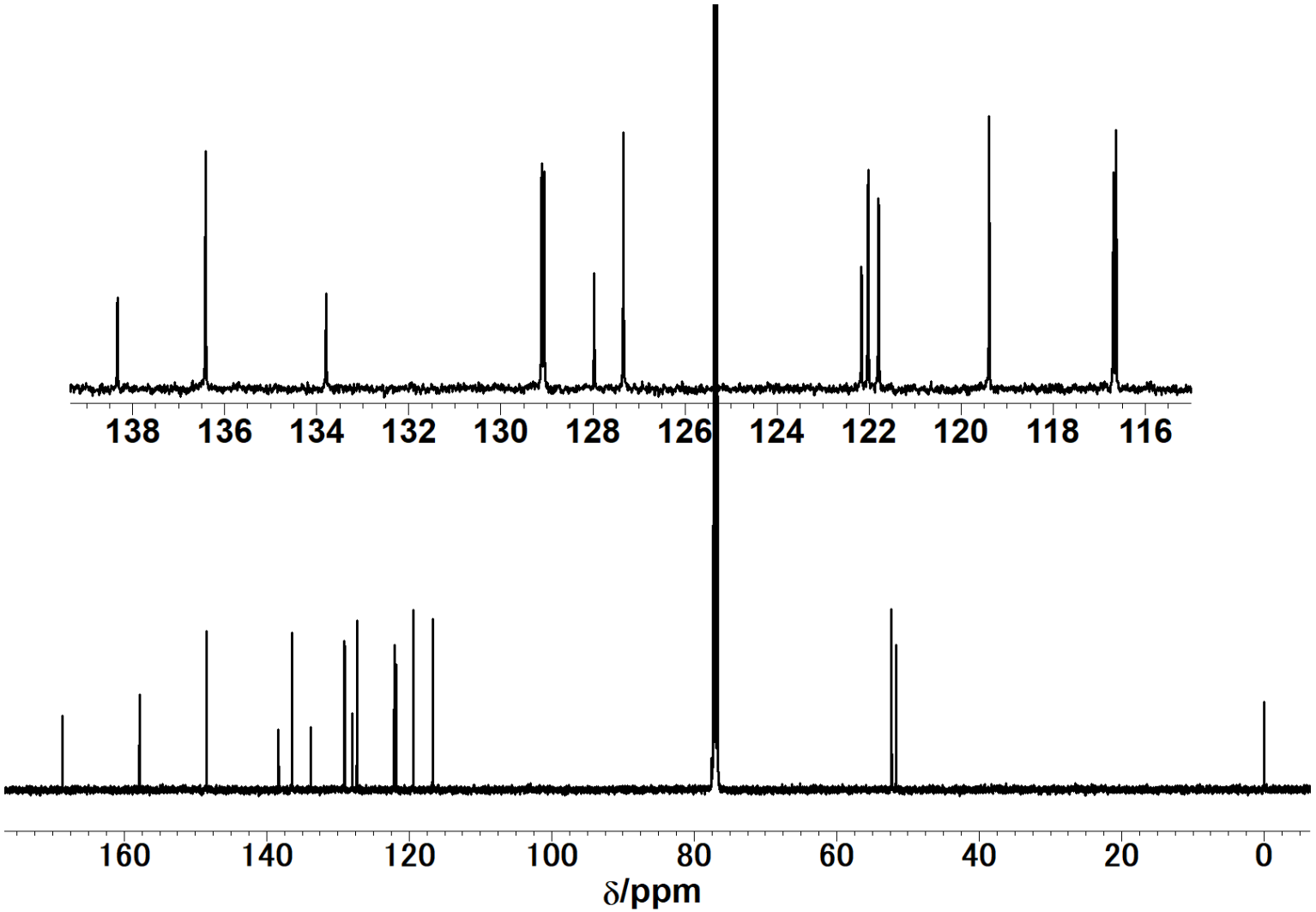

Figure S2. ^{13}C NMR spectrum of **1** in $CDCl_3$.

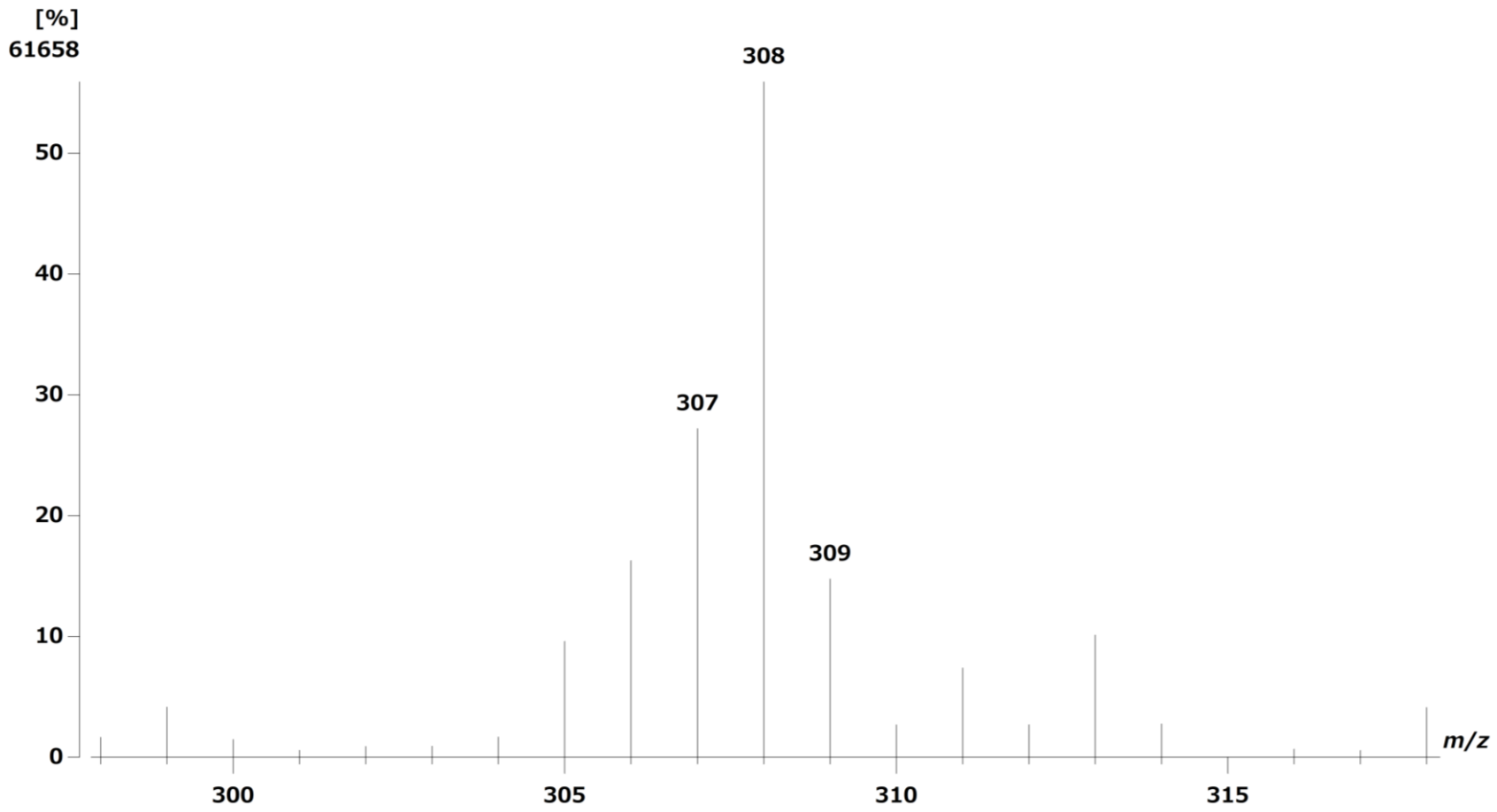

Figure S3. FAB mass spectrum (positive mode) of **1**.

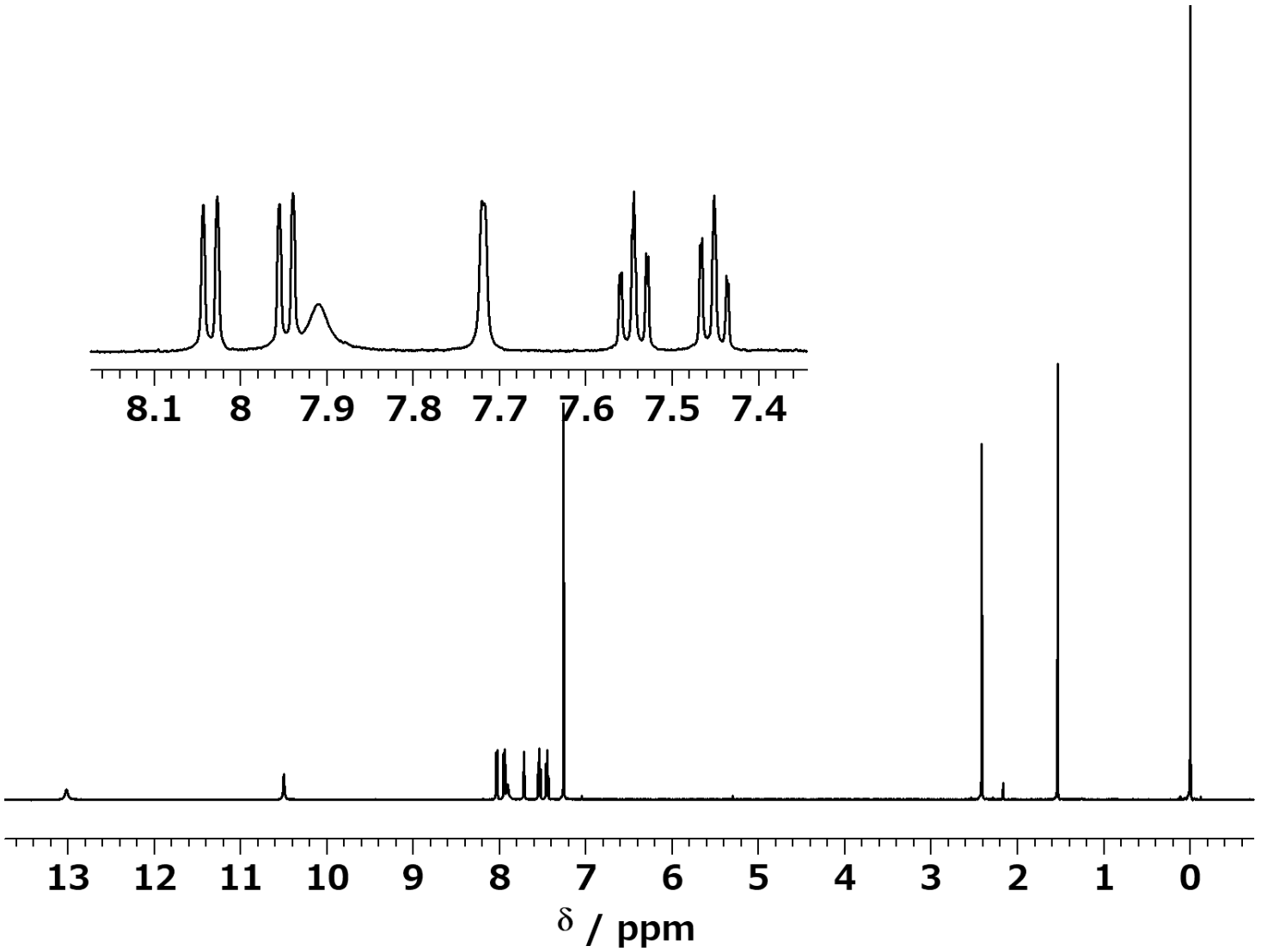

Figure S4. ^{1}H NMR spectrum of compound **9** in $CDCl_3$.

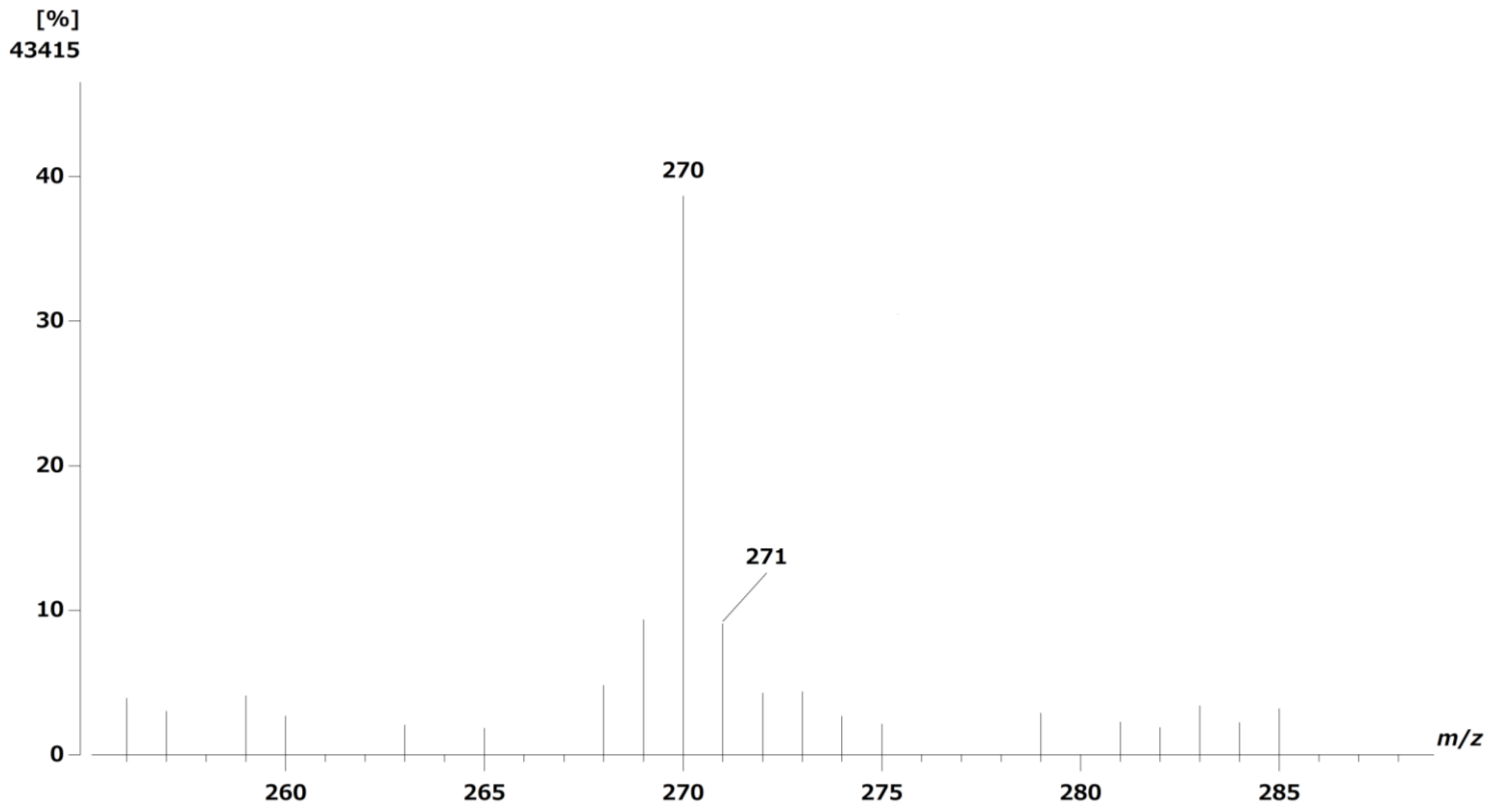

Figure S5. FAB mass spectrum (positive mode) of **9**.

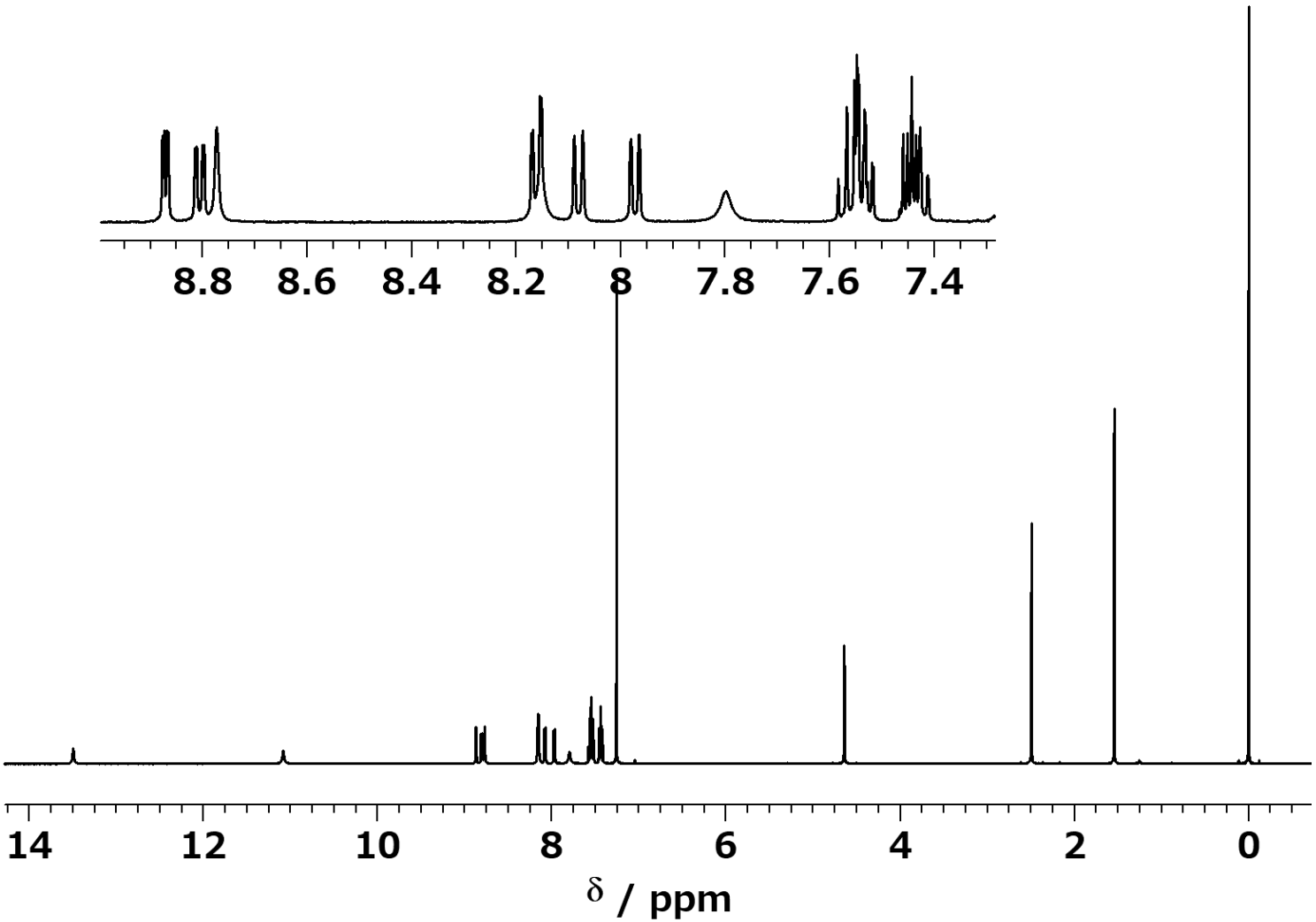

Figure S6. ^{1}H NMR spectrum of **2** in $CDCl_3$.

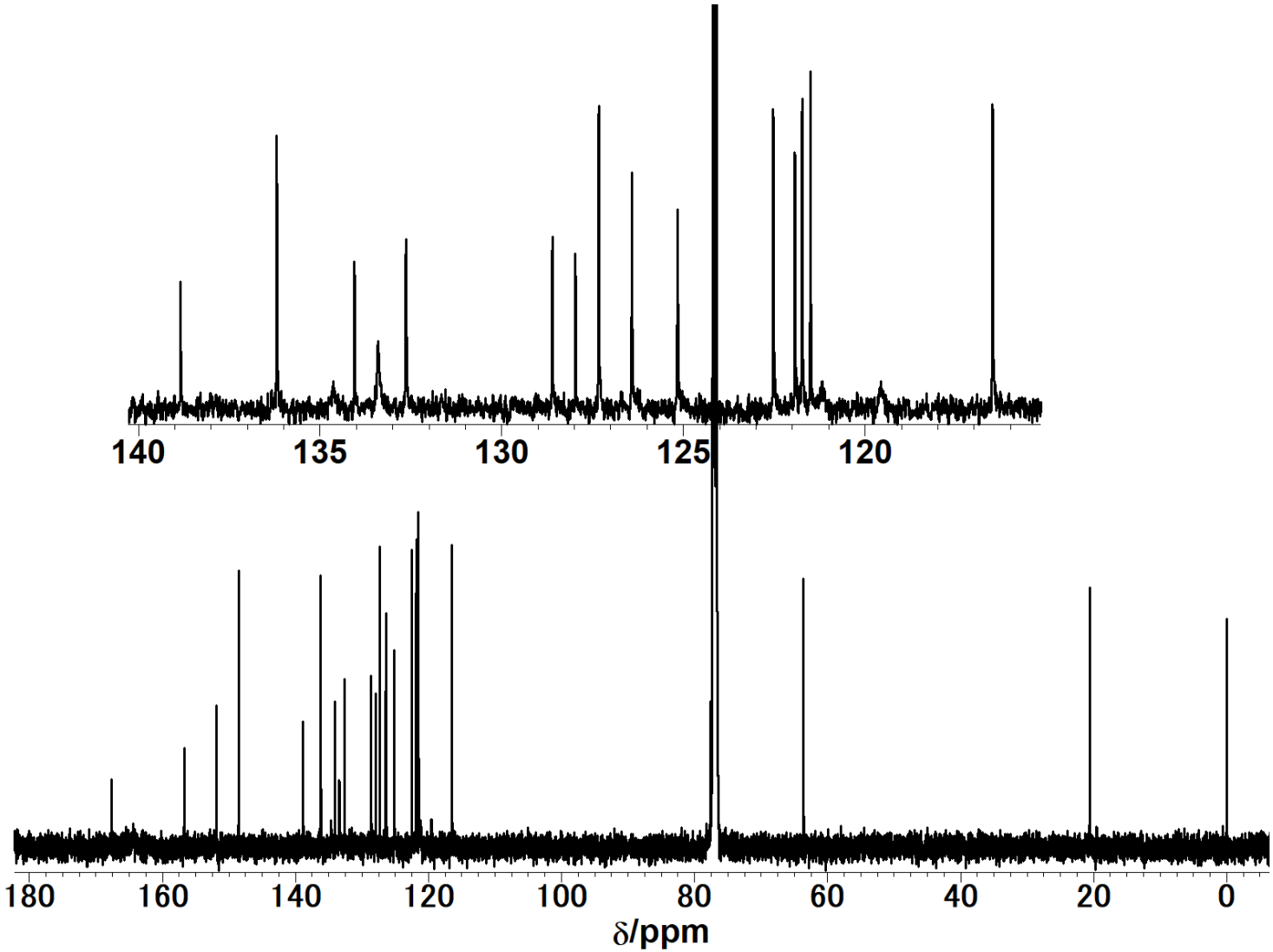

Figure S7. ^{13}C NMR spectrum of **2** in $CDCl_3$.

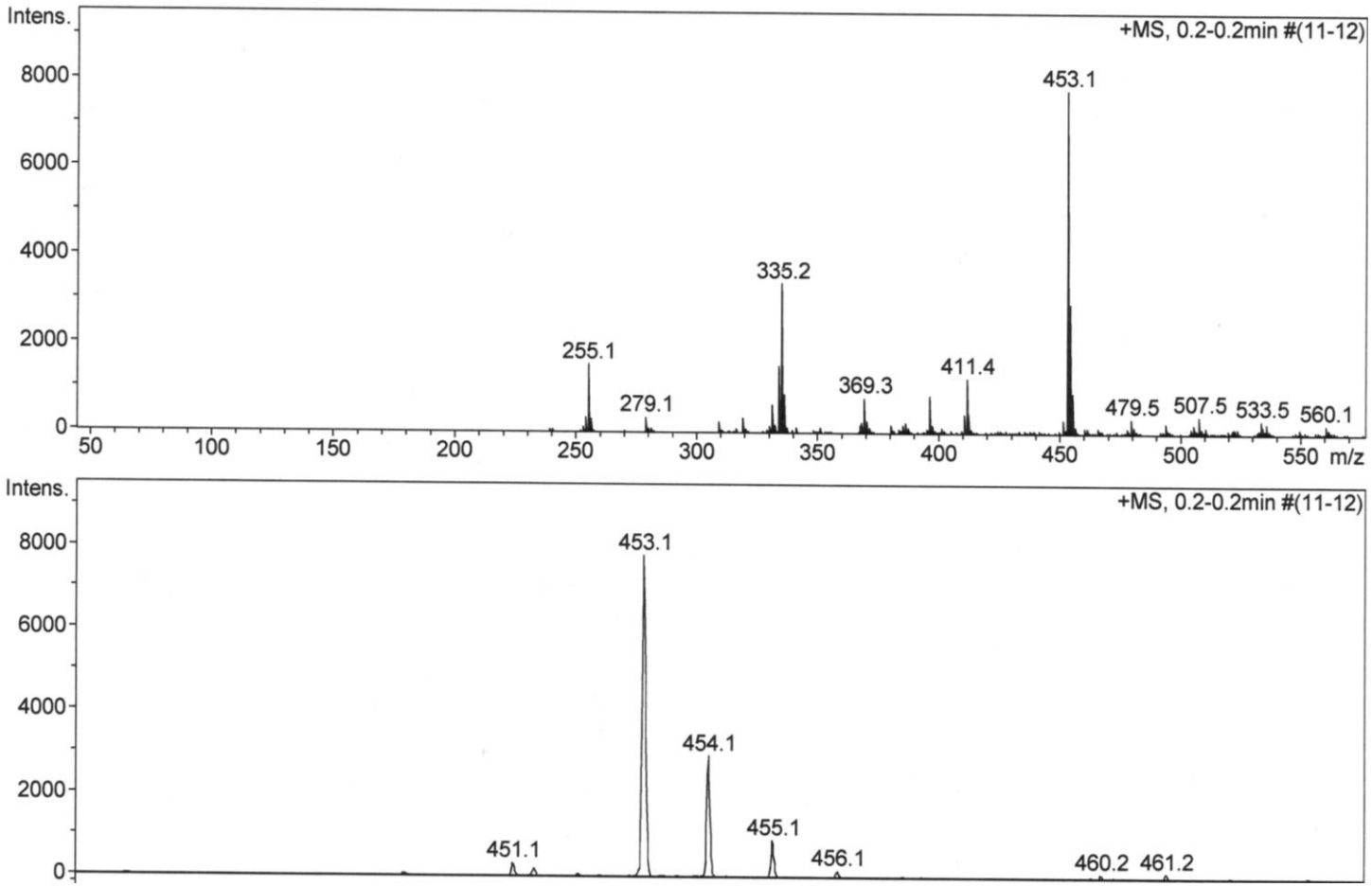

Figure S8. APCI mass spectrum (positive mode) of **2**.

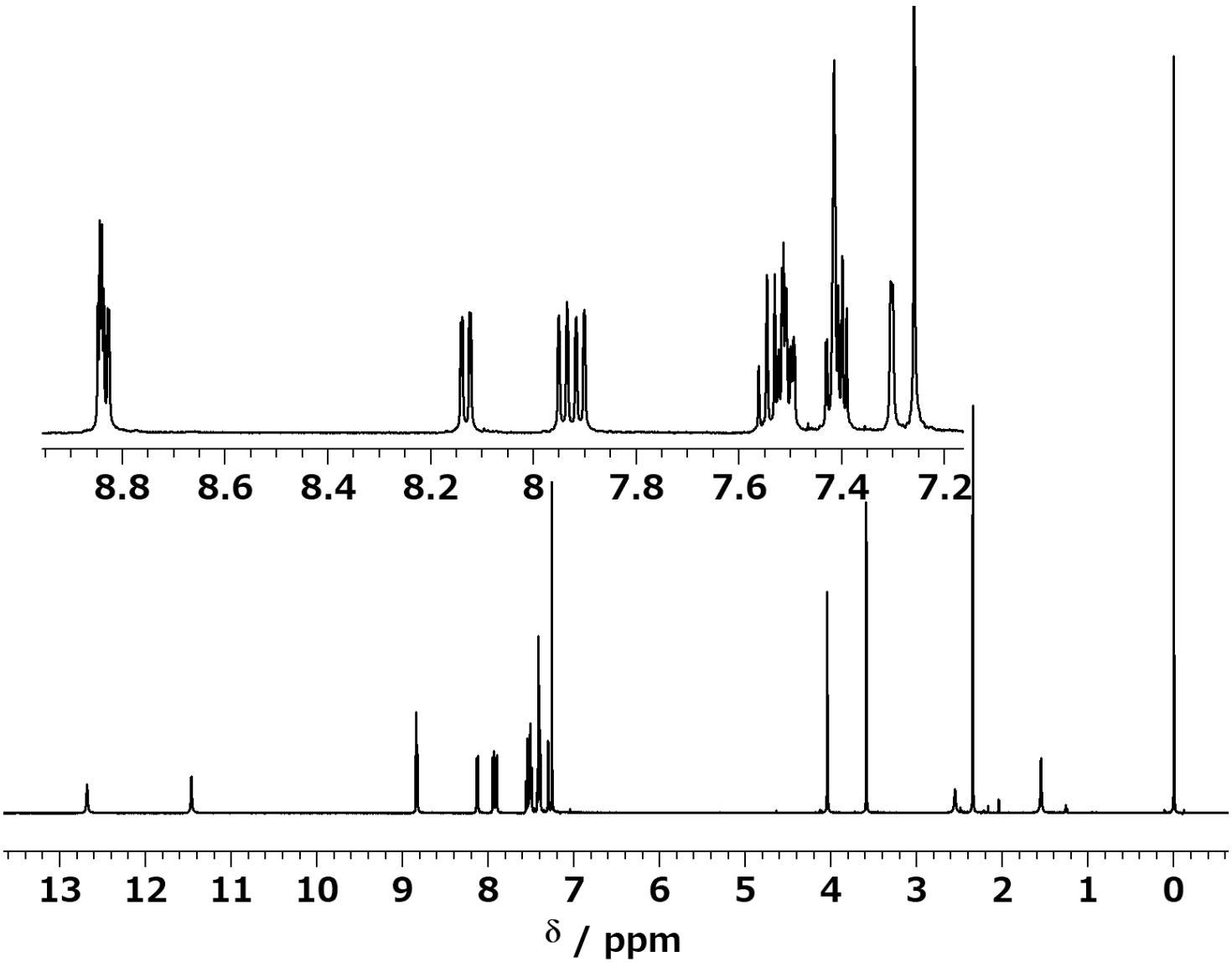

Figure S9. ^{1}H NMR spectrum of **3** in $CDCl_3$.

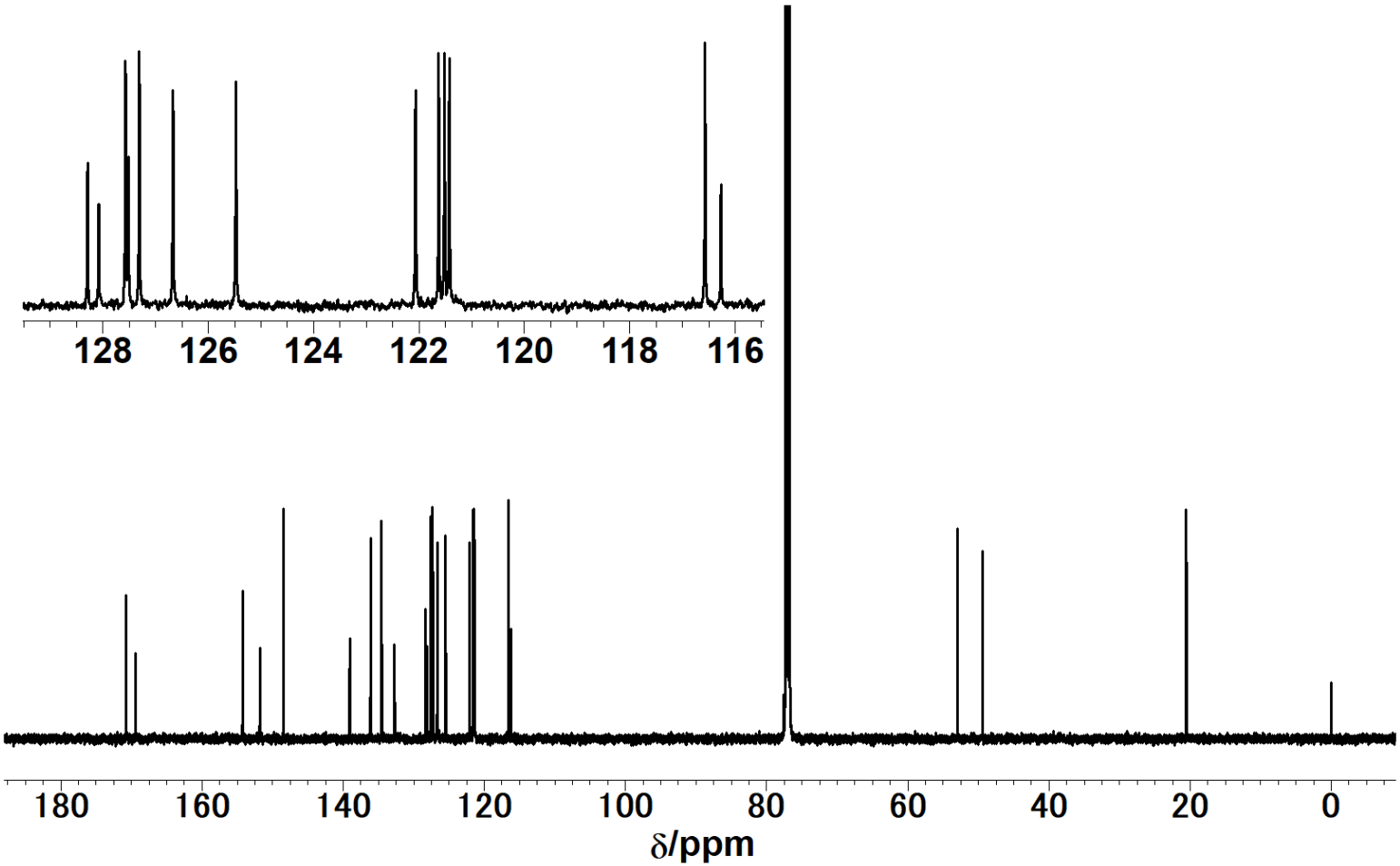

Figure S10. ^{13}C NMR spectrum of **3** in $CDCl_3$.

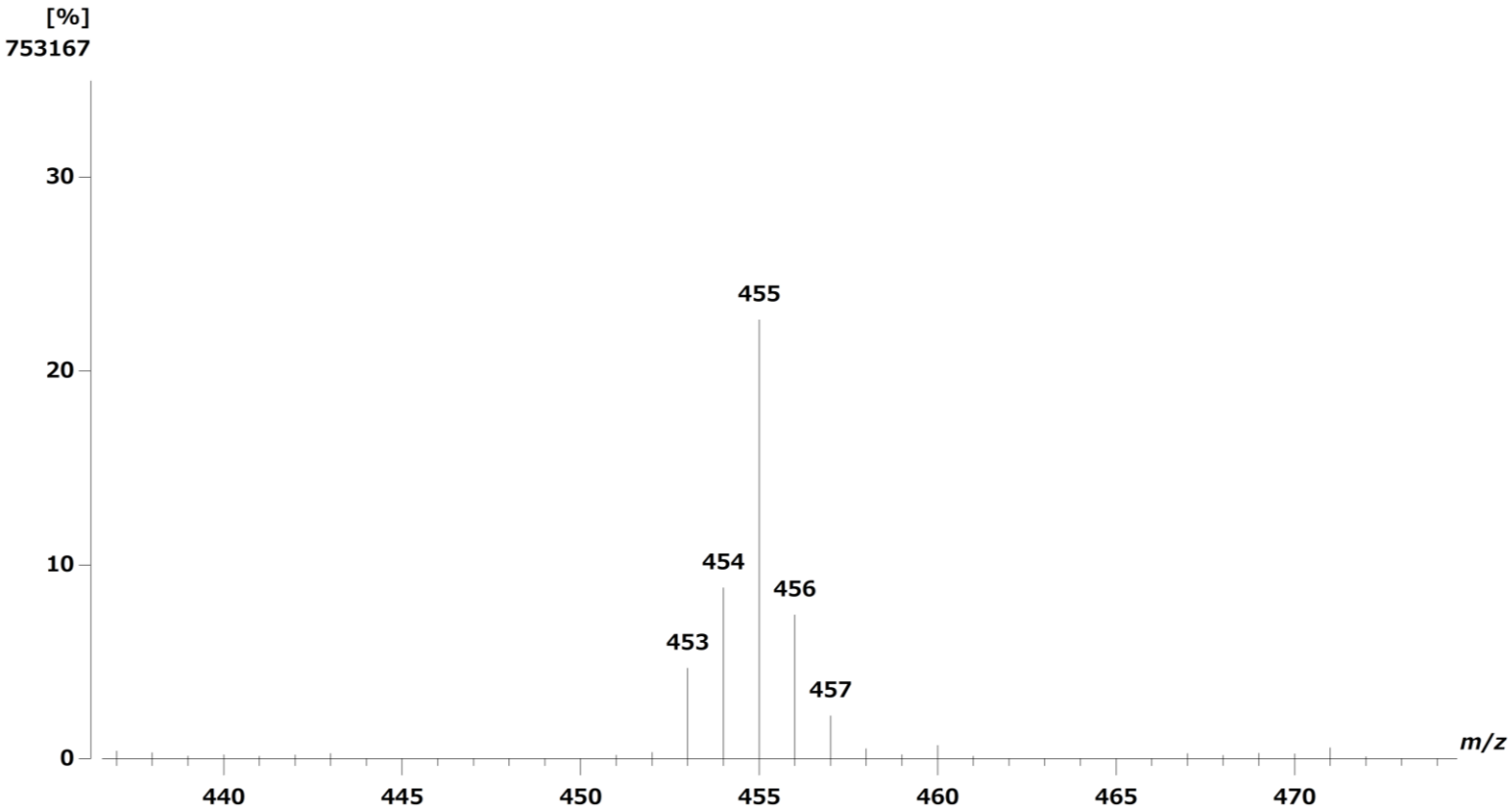

Figure S11. FAB mass spectrum (positive mode) of **3.**

4. UV-Vis titrations of ligands with metal ion

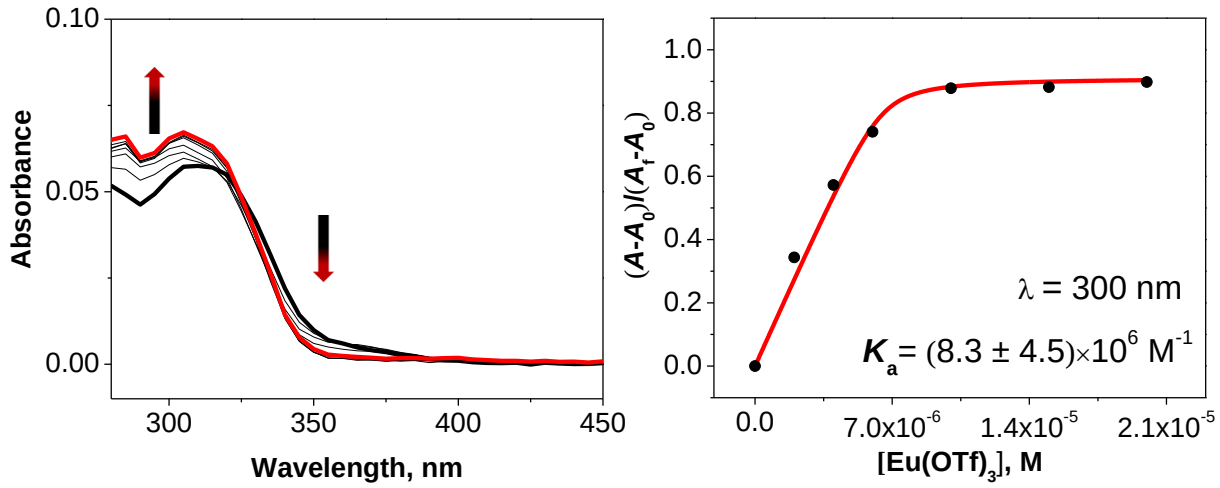

Figure S12: UV-Vis titration and isotherm of **1** (10 μM) upon the addition of $Eu(OTf)_3$ in MeOH (0.2% DMSO).

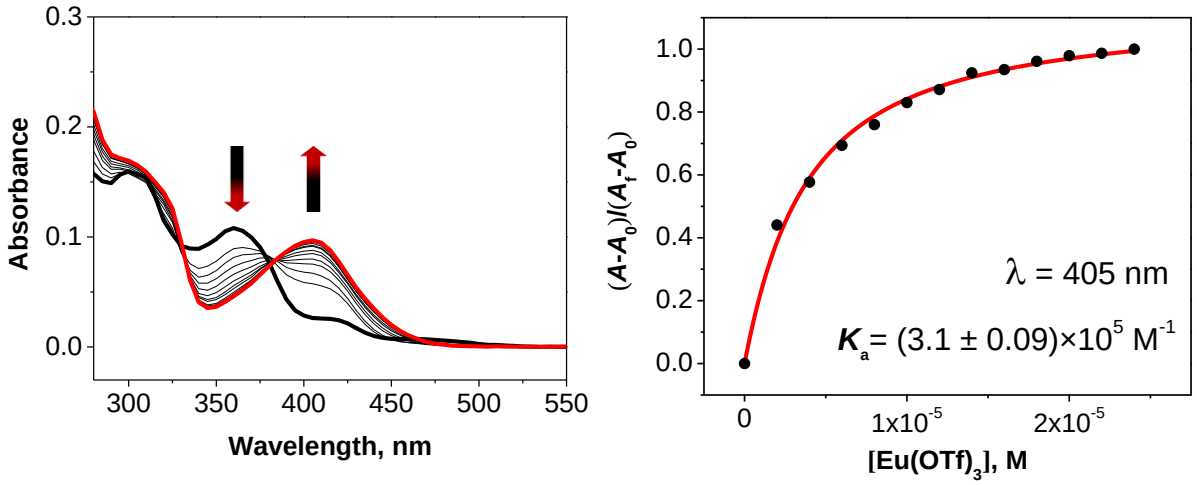

Figure S13: UV-Vis titration and isotherm of **2** (10 μM) upon the addition of $Eu(OTf)_3$ in MeOH (2.5% DMSO).

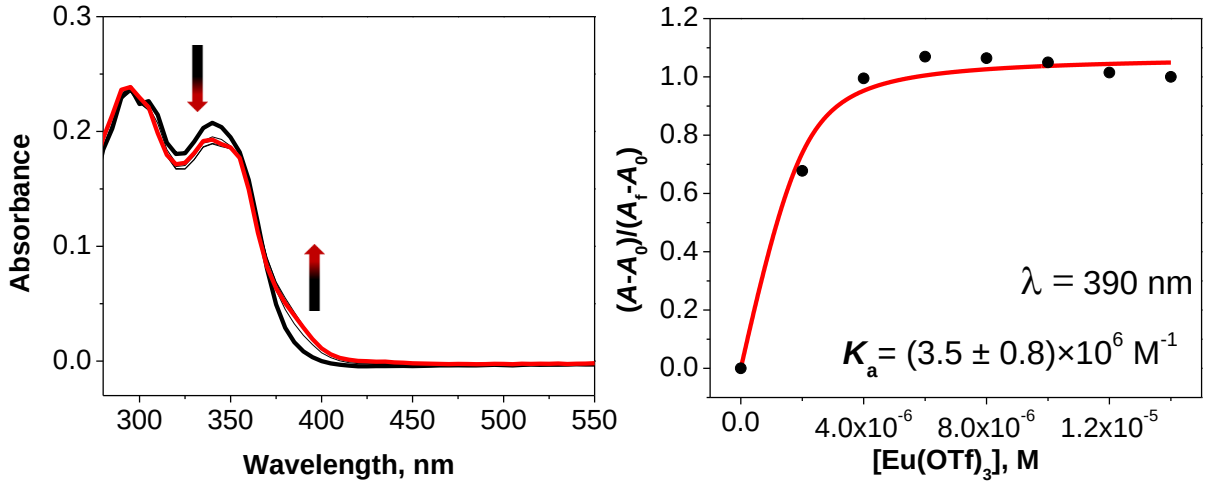

Figure S14: UV-Vis titration and isotherm of **3** (10 μM) upon the addition of $Eu(OTf)_3$ in MeOH (2.5% DMSO).

5. Fluorescence titrations of ligands with metal ion

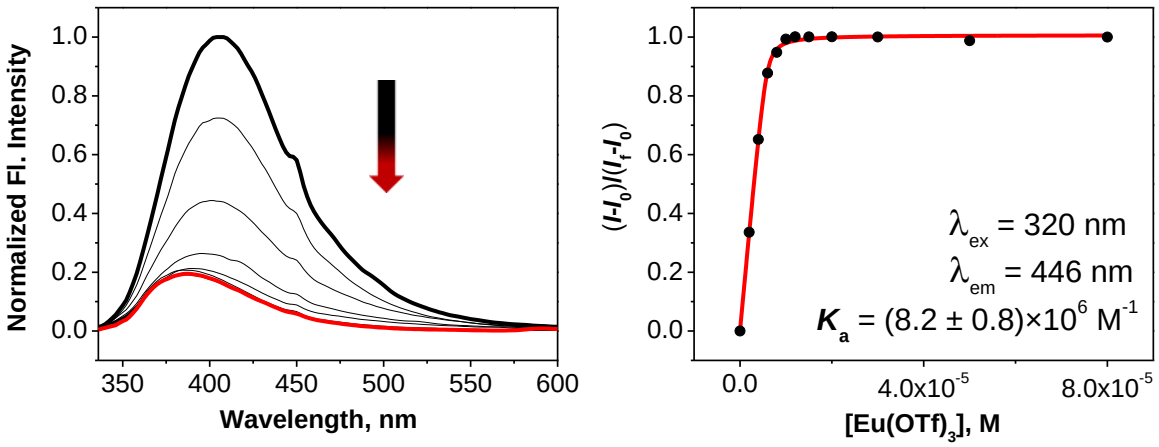

Figure S15: Fluorescence titrations and isotherm of **1** (10 μM) upon the addition of $Eu(OTf)_3$ in MeOH (0.2% DMSO).

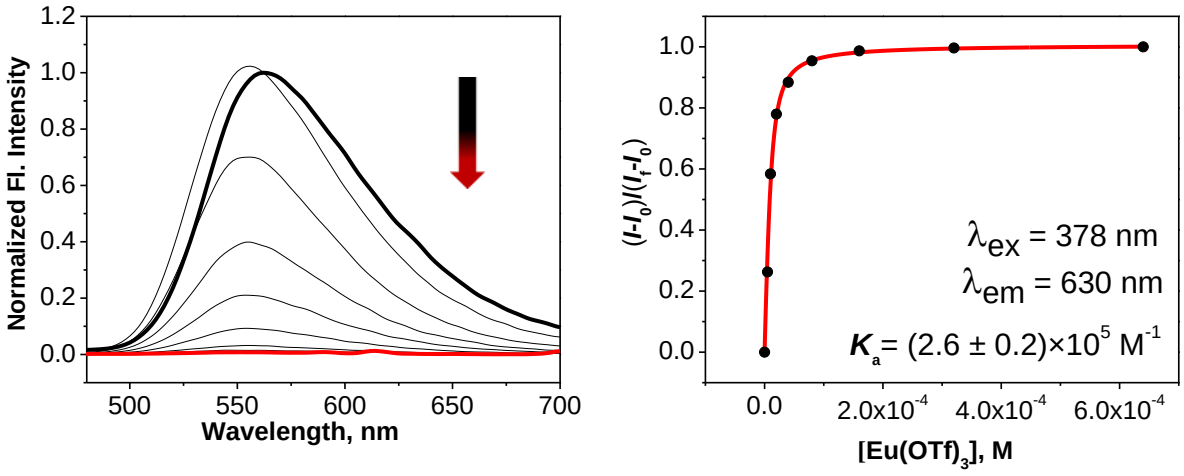

Figure S16: Fluorescence titrations and isotherm of **2** (10 μM) upon the addition of $Eu(OTf)_3$ in MeOH (2.5% DMSO).

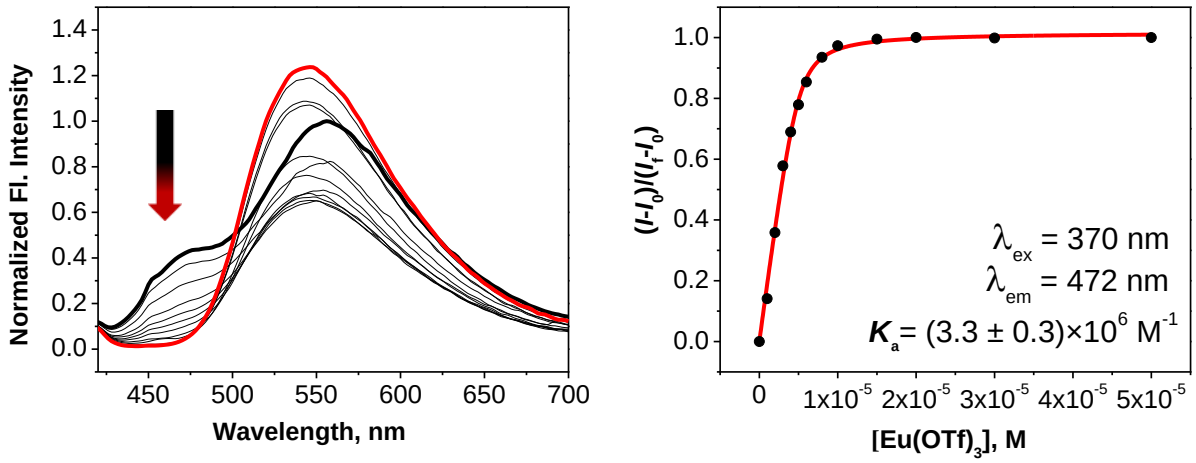

Figure S17: Fluorescence titrations and isotherm of **3** (10 μM) upon the addition of $Eu(OTf)_3$ in MeOH (2.5% DMSO).

6. Fluorescence titrations of ensembles with analytes

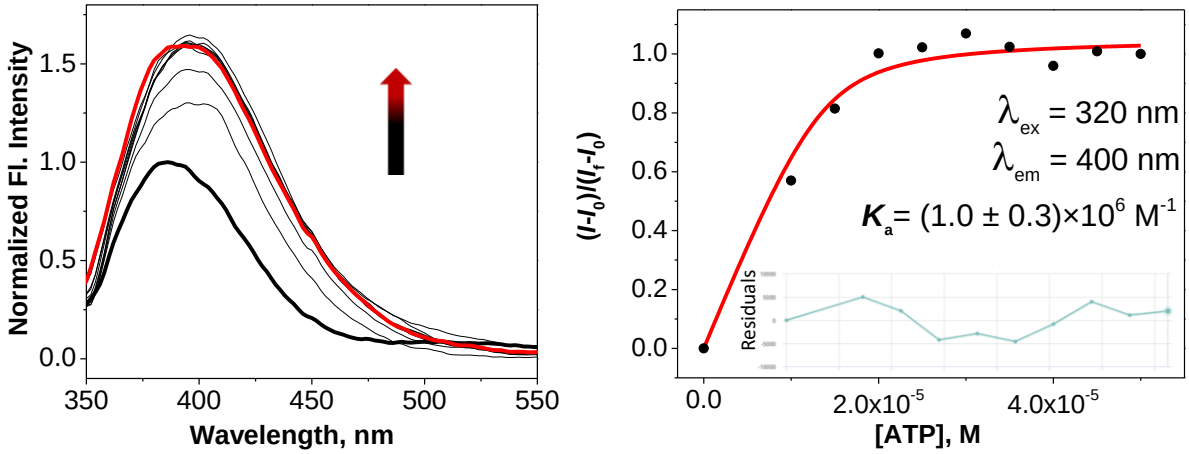

Figure S18: Fluorescence titration spectra and isotherm of [**1**-Eu] ([**1**] = 10.0 μM, [$Eu(OTf)_3$] = 10.0 μM) upon the addition of incremental amount of ATP, [0-50] μM, in MeOH.

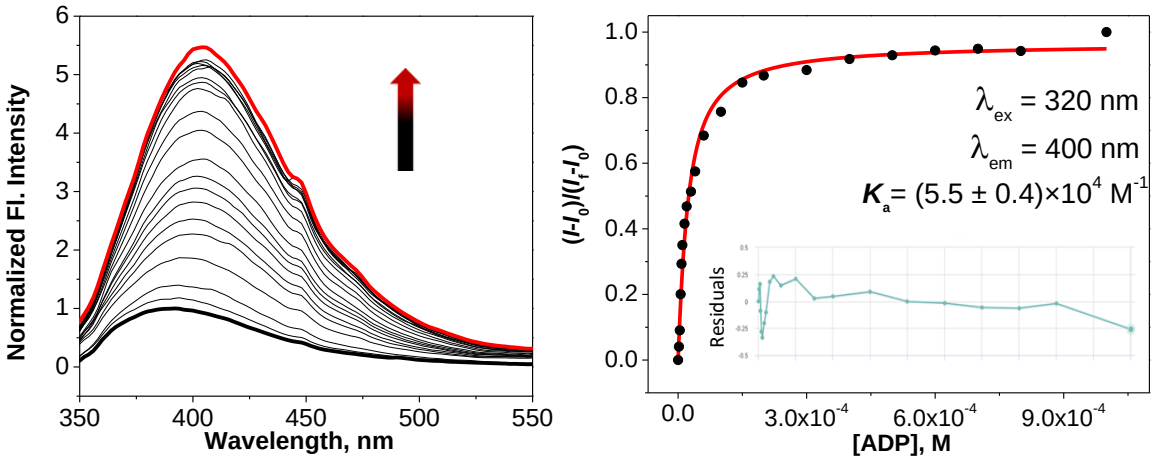

Figure S19: Fluorescence titration spectra and isotherm of [**1**-Eu] ([**1**] = 10.0 μM, [$Eu(OTf)_3$] = 10.0 μM) upon the addition of incremental amount of ADP, [0-1000] μM, in MeOH.

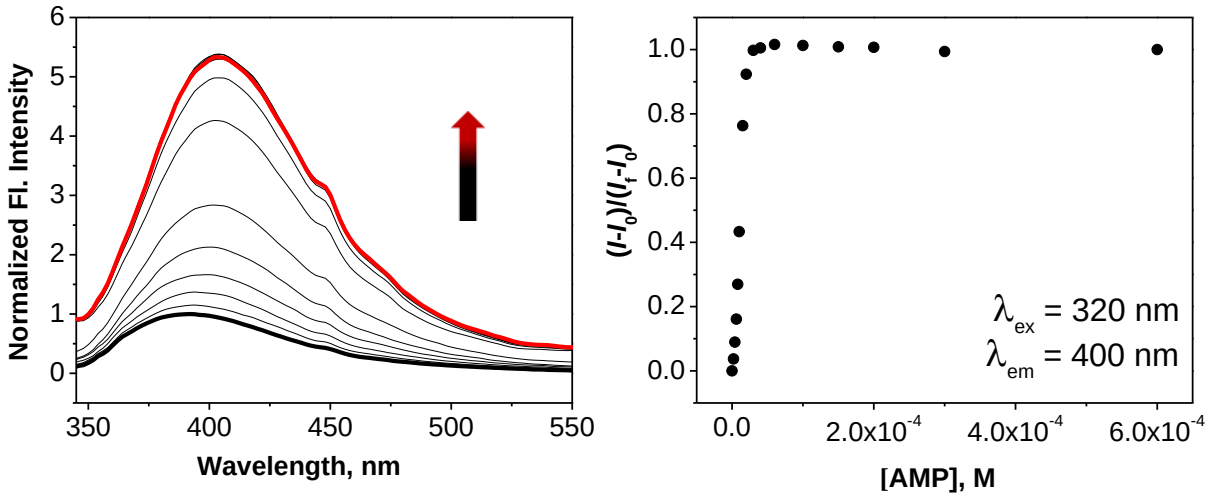

Figure S20: Fluorescence titration spectra and isotherm of [**1**-Eu] ([**1**] = 10.0 μM, [Eu(OTf)3] = 10.0 μM) upon the addition of incremental amount of AMP, [0-600] μM, in MeOH. Constant could not be determined due to multiple equilibria that appear to be involved.

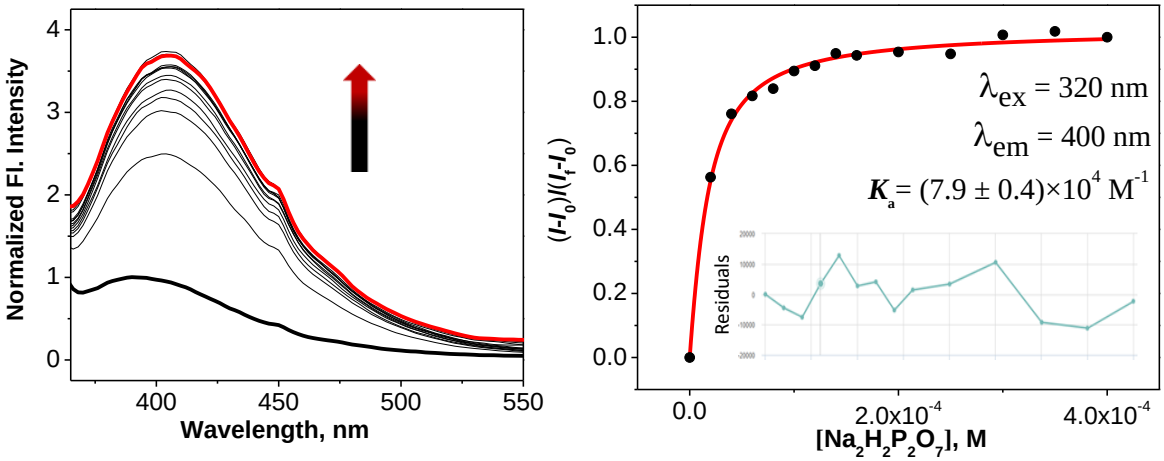

Figure S21: Fluorescence titration spectra and isotherm of [**1**-Eu] ([**1**] = 10.0 μM, [Eu(OTf)3] = 10.0 μM) upon the addition of incremental amount of $Na_2H_2P_2O_7$, [0-400] μM, in MeOH.

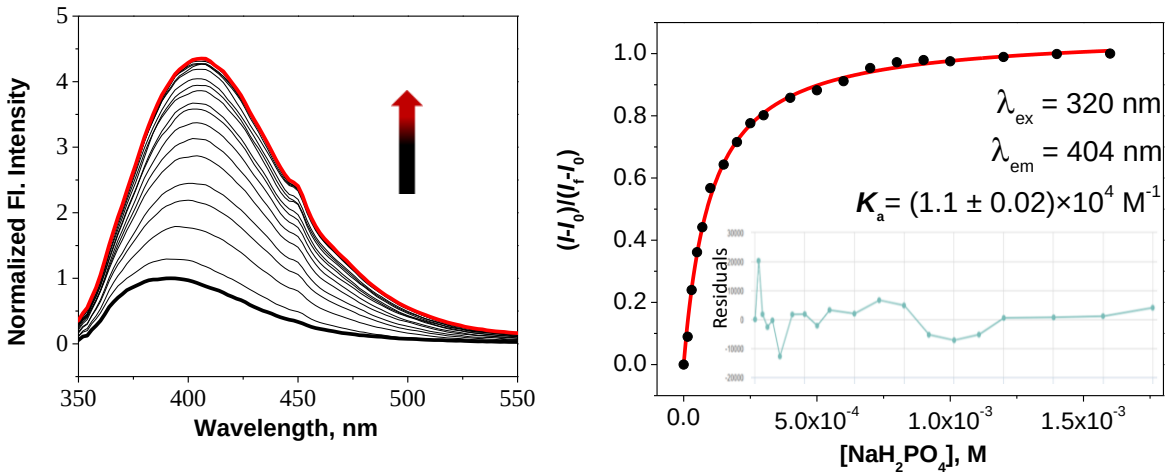

Figure S22: Fluorescence titration spectra and isotherm of [**1**-Eu] ([**1**] = 10.0 μM, [Eu(OTf)$_3$] = 10.0 μM) upon the addition of incremental amount of NaH_2PO_4, [0-1600] μM, in MeOH.

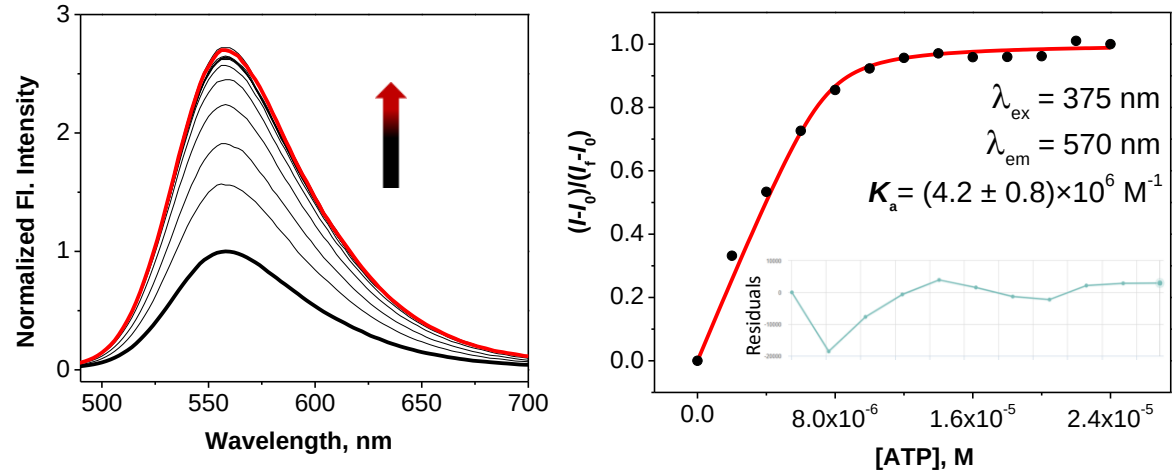

Figure S23: Fluorescence titration spectra and isotherm of [**2**-Eu] ([**2**] = 10.0 μM, [Eu(OTf)$_3$] = 10.0 μM) upon the addition of incremental amount of ATP, [0-24] μM, in MeOH (2.5% DMSO).

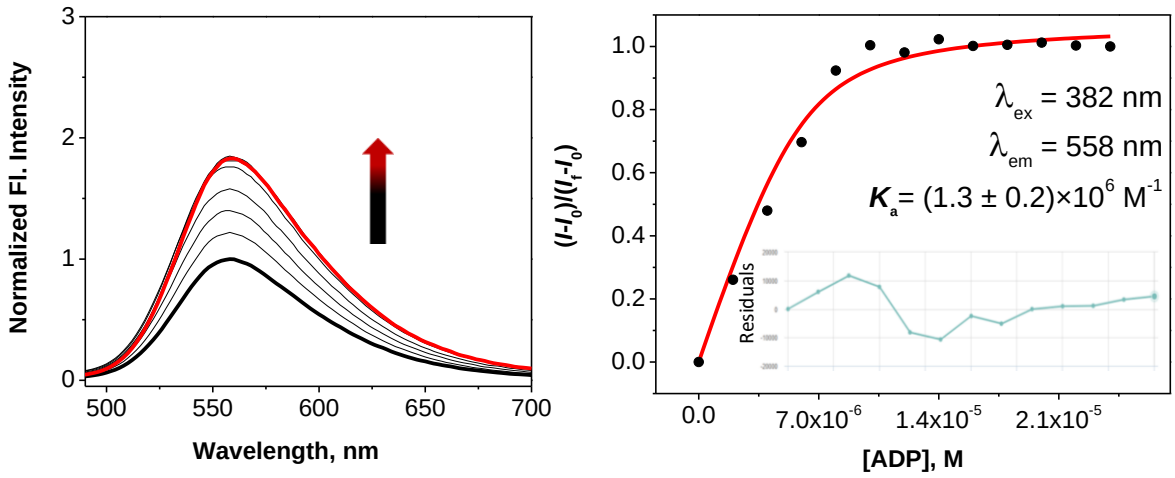

Figure S24: Fluorescence titration spectra and isotherm of [**2**-Eu] ([**2**] = 10.0 μM, [Eu(OTf)$_3$] = 10.0 μM) upon the addition of incremental amount of ADP, [0-24] μM, in MeOH (2.5% DMSO).

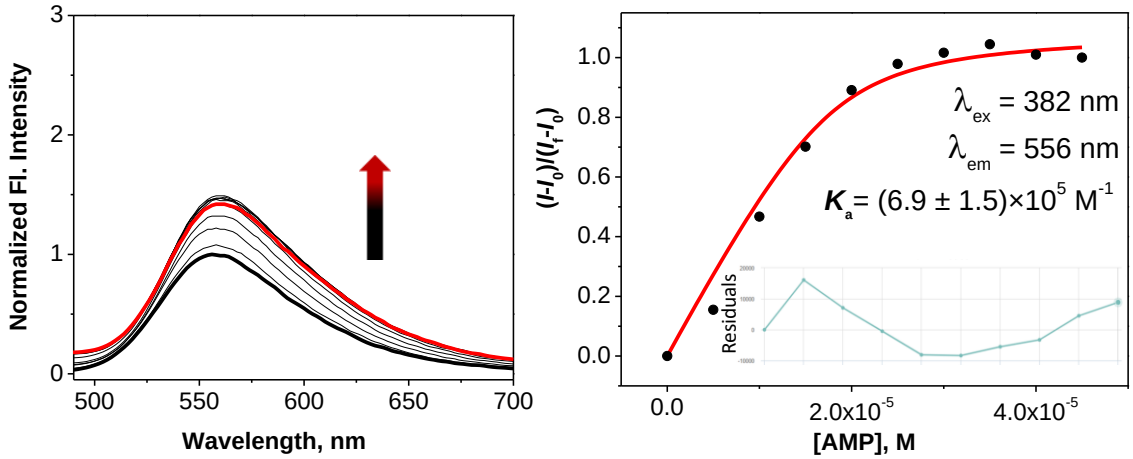

Figure S25: Fluorescence titration spectra and isotherm of [**2**-Eu] ([**2**] = 10.0 μM, [Eu(OTf)$_3$] = 10.0 μM) upon the addition of incremental amount of AMP, [0-50] μM, in MeOH (2.5% DMSO).

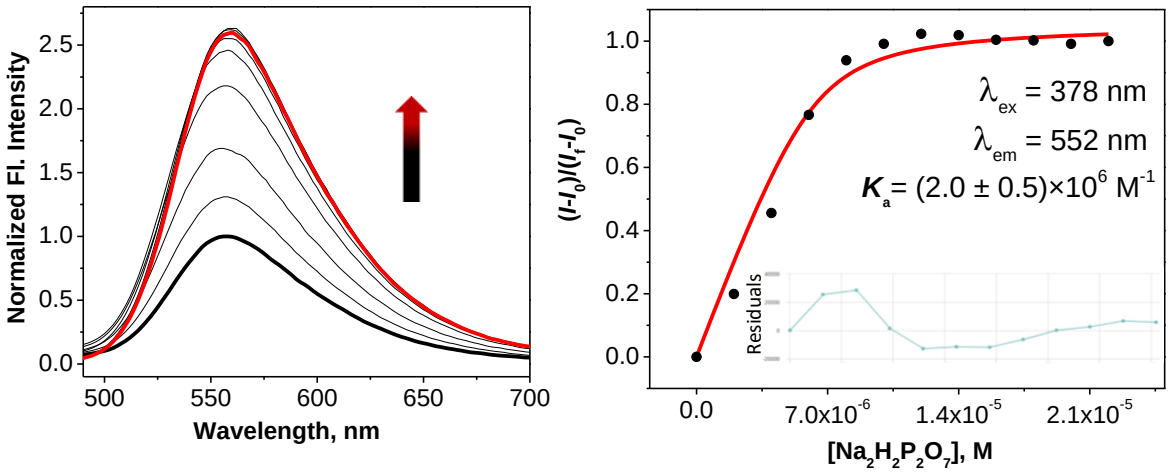

Figure S26: Fluorescence titration spectra and isotherm of [**2**-Eu] ([**2**] = 10.0 µM, [Eu(OTf)$_3$] = 10.0 µM) upon the addition of incremental amount of $Na_2H_2P_2O_7$, [0-22] µM, in MeOH (2.5% DMSO).

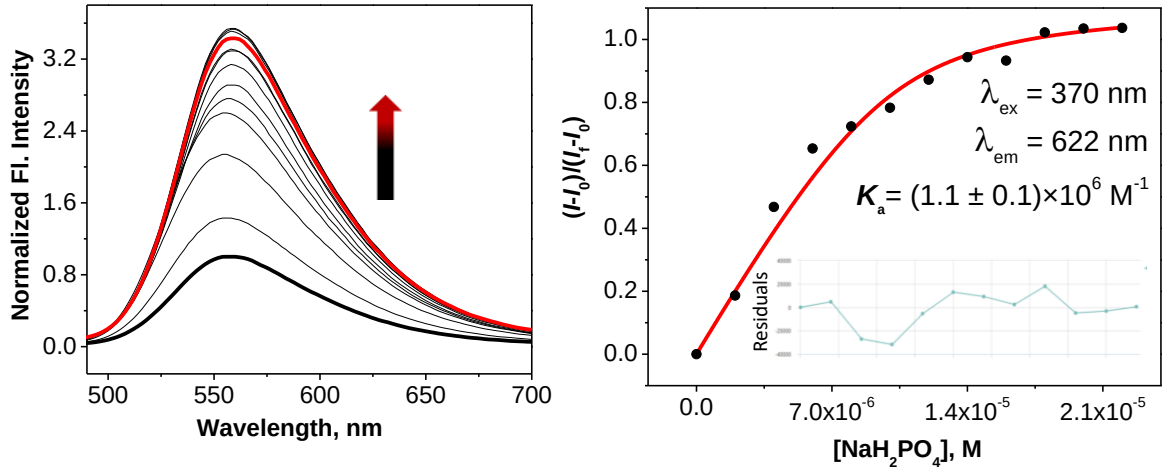

Figure S27: Fluorescence titration spectra and isotherm of [**2**-Eu] ([**2**] = 10.0 µM, [Eu(OTf)$_3$] = 10.0 µM) upon the addition of incremental amount of NaH_2PO_4, [0-24] µM, in MeOH (2.5% DMSO)..

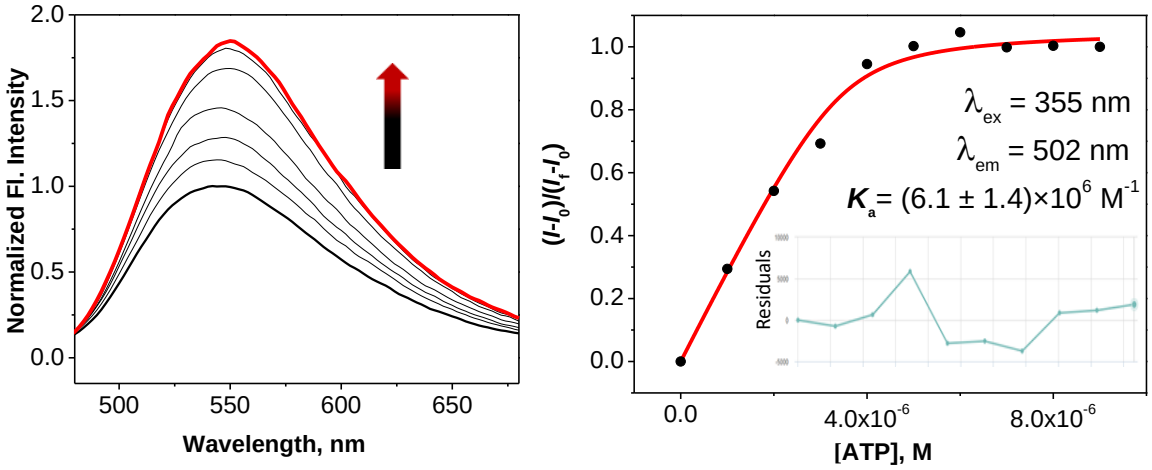

Figure S28: Fluorescence titration spectra and isotherm of [**3**-Eu] ([**3**] = 10.0 μM, [$Eu(OTf)_3$] = 10.0 μM) upon the addition of incremental amount of ATP, [0-10] μM, in MeOH (2.5% DMSO).

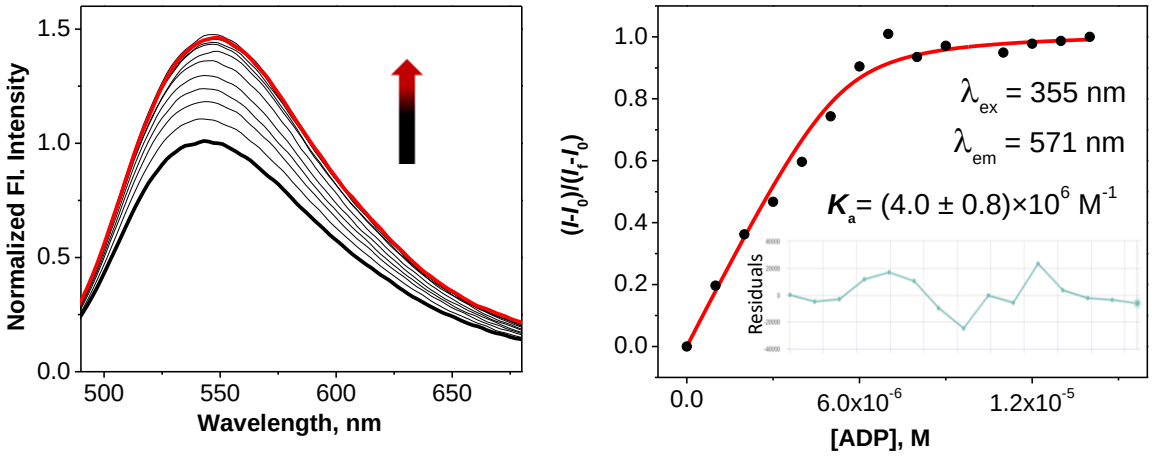

Figure S29: Fluorescence titration spectra and isotherm of [**3**-Eu] ([**3**] = 10.0 μM, [$Eu(OTf)_3$] = 10.0 μM) upon the addition of incremental amount of ADP, [0-14] μM, in MeOH (2.5% DMSO).

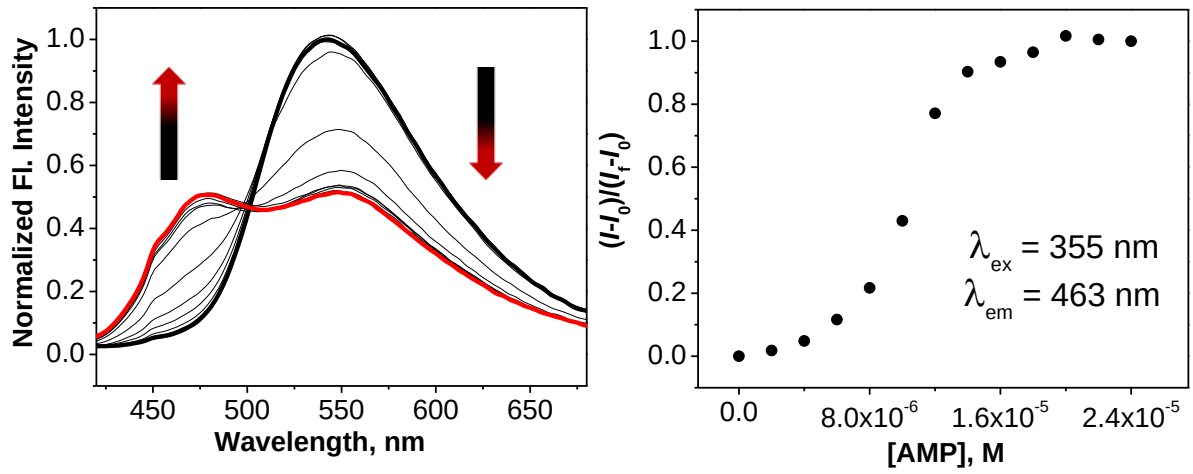

Figure S30: Fluorescence titration spectra and isotherm of [**3**-Eu] ([**3**] = 10.0 μM, [Eu(OTf)$_3$] = 10.0 μM) upon the addition of incremental amount of AMP, [0-24] μM, in MeOH (2.5% DMSO). Constant could not be determined due to multiple equilibria that appear to be involved.

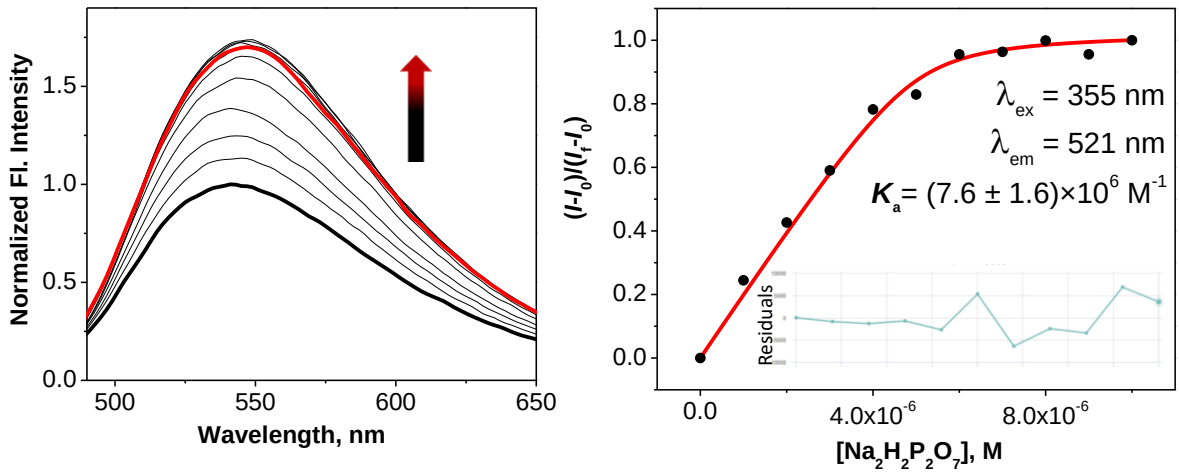

Figure S31: Fluorescence titration spectra and isotherm of [**3**-Eu] ([**3**] = 10.0 μM, [Eu(OTf)$_3$] = 10.0 μM) upon the addition of incremental amount of $Na_2H_2P_2O_7$, [0-10] μM, in MeOH (2.5% DMSO).

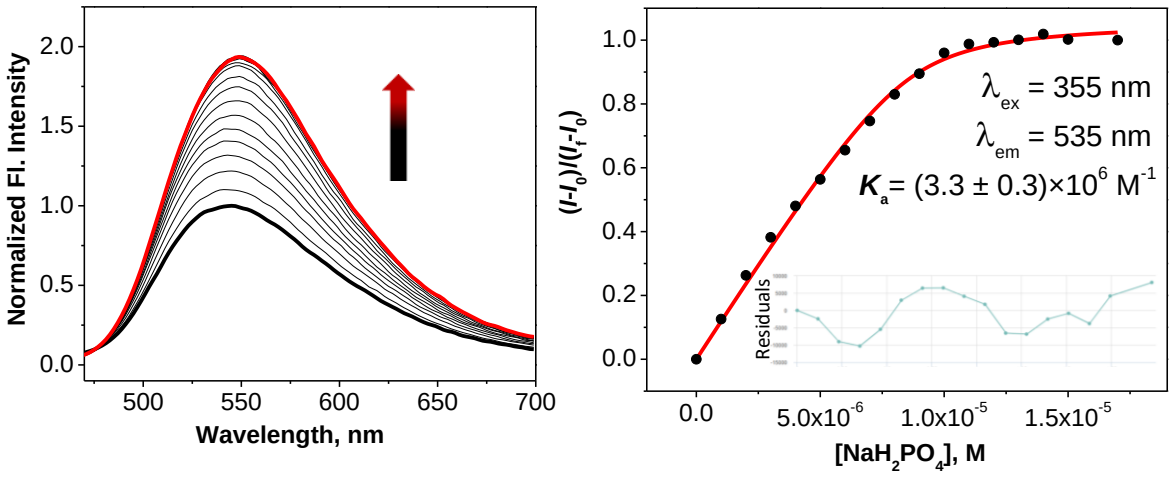

Figure S32: Fluorescence titration spectra and isotherm of [**3**-Eu] ([**3**] = 10.0 μM, [Eu(OTf)$_3$] = 10.0 μM) upon the addition of incremental amount of NaH_2PO_4, [0-17] μM, in MeOH (2.5% DMSO).

7. Job Plot stoichiometry determination

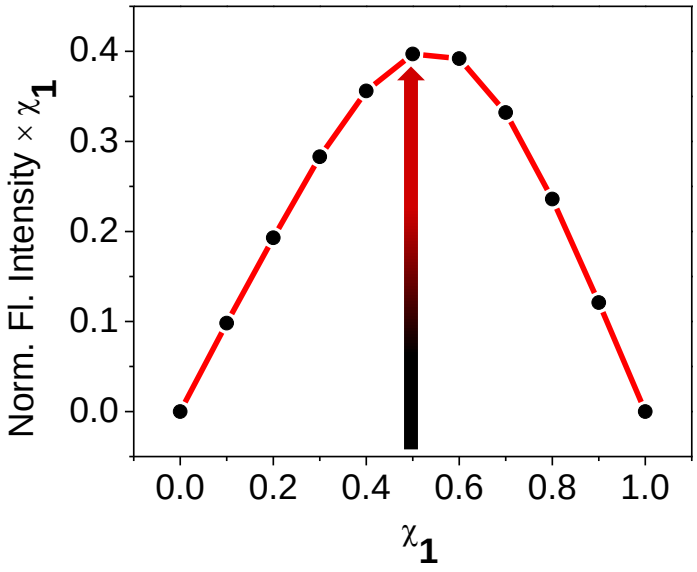

Figure S33: The Job plot from fluorescence titration of **1** upon the addition of Eu(OTf)$_3$ in MeOH (0.2% DMSO).

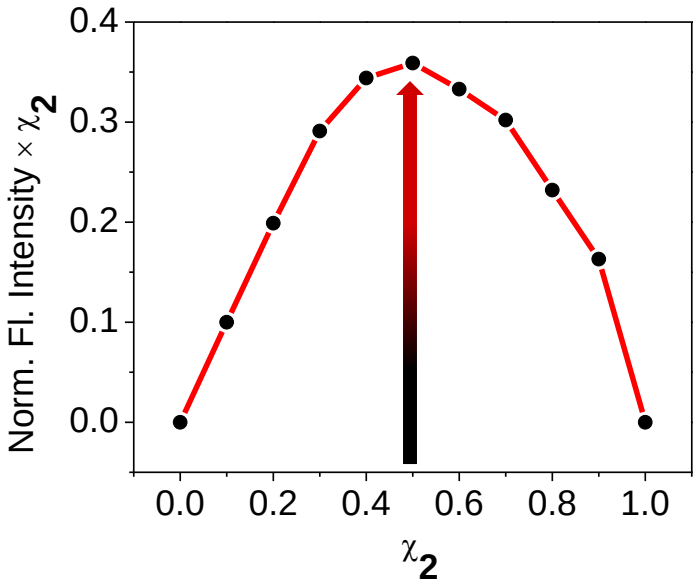

Figure S34: The Job plot from fluorescence titration of **2** upon the addition of $Eu(OTf)_3$ in MeOH (2.5% DMSO).

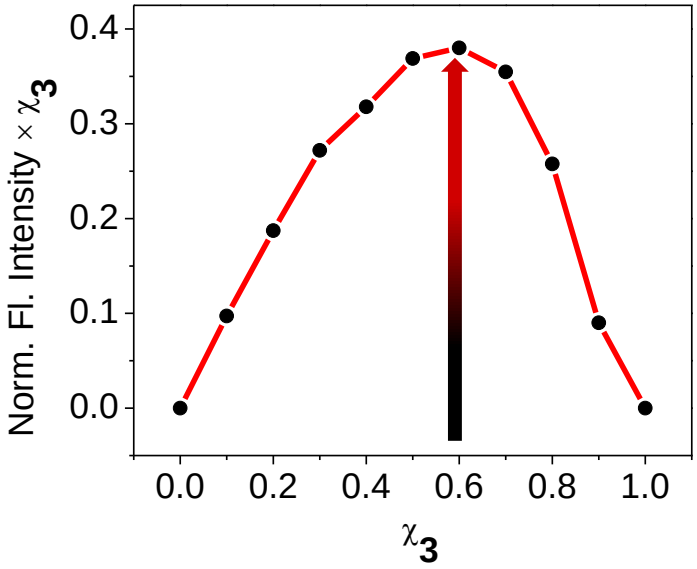

Figure S35: The Job plot from fluorescence titration of **3** upon the addition of $Eu(OTf)_3$ in MeOH (2.5% DMSO).

8. Absolute Quantum Yield Determination

Ligands	$\lambda_{A,\,max}$ (nm)	Φ^{a} (%)
1	313 nm	1.2%
2	315 nm	12.1%
3	338 nm	3.8%

[a] Absolute quantum yields were determined upon excitation at indicated wavelength ($\lambda_{A,\,max}$) for solutions with optical density A < 0.1. All measurements were carried out in pure DMSO.

9. Fourier-Transform Infrared (FTIR) Spectra

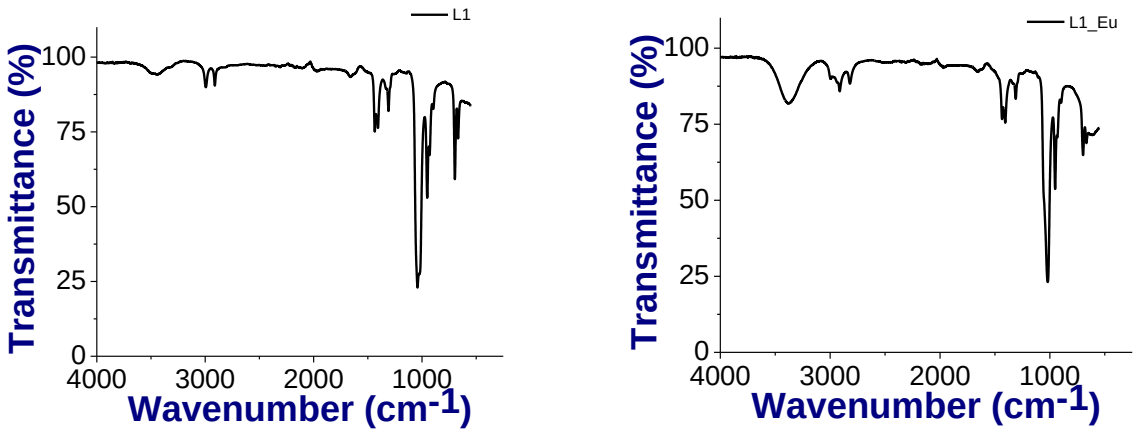

Figure S36: FTIR spectra of **1** (left) and [**1**-Eu] (Right) in MeOH.

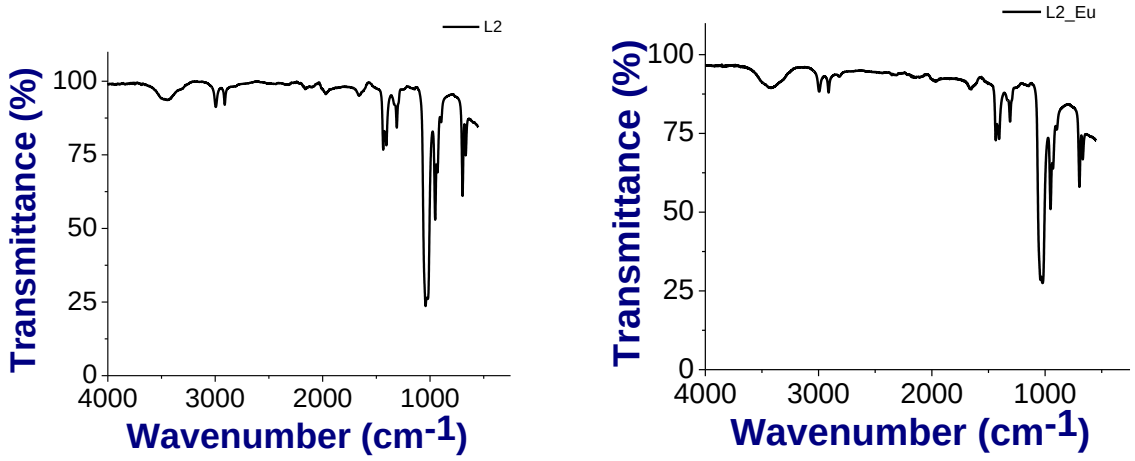

Figure S37: FTIR spectra of **2** (left) and [**2**-Eu] (Right) in MeOH.

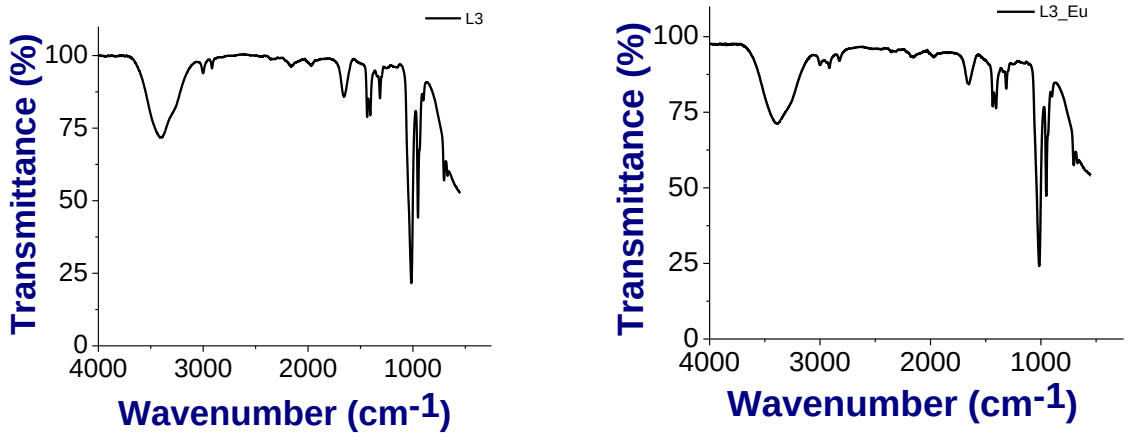

Figure S37: FTIR spectra of **3** (left) and [**3**-Eu] (Right) in MeOH.

10. References

1 M. Pushina, S. Farshbaf, W. Mochida, M. Kanakubo, R. Nishiyabu, Y. Kubo and P. Anzenbacher Jr., *Chem. - Eur. J.*, 2021, **27**, 11344–11351.

2 J. Zhang, X. Wang, C. Tu, J. Lin, J. Ding, L. Lin, Z. Wang, C. He, C. Yan, X. You and Z. Guo, *J. Med. Chem.*, 2003, **46**, 3502–3507.

3 J. Li, Y. Chen, T. Chen, J. Qiang, Z. Zhang, T. Wei, W. Zhang, F. Wang and X. Chen, *Sens. Actuators, B*, 2018, **268**, 446–455.